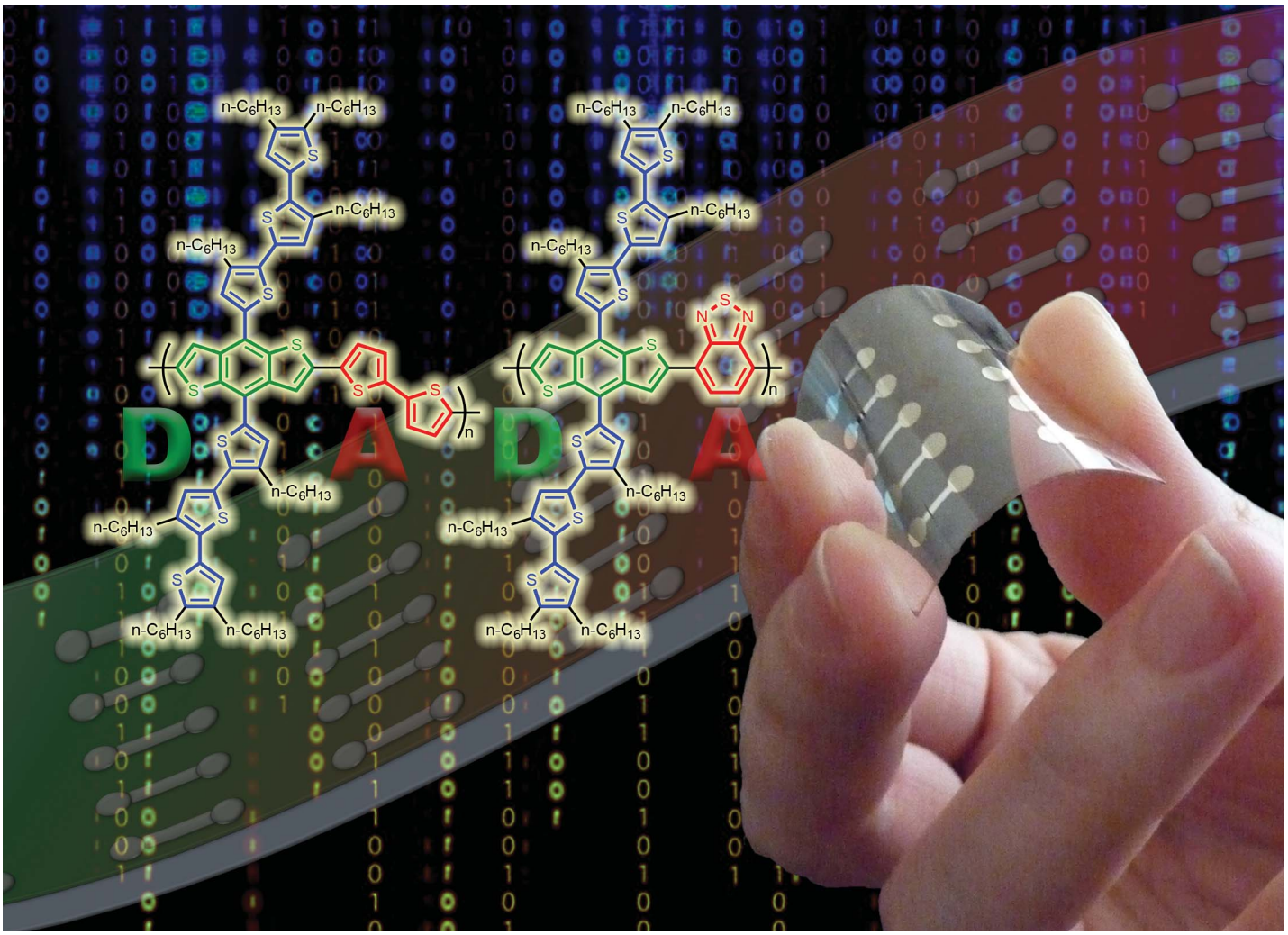

Showcasing cooperative research from Physical Chemistry and Applied Spectroscopy (C-PCS), Material Synthesis and Integrated Devices (MPA-11), and Materials Science in Radiation & Dynamics (MST-8) at Los Alamos National Laboratory and the Institute of Polymer Science and Engineering at National Taiwan University.

Title: Flexible memory devices with tunable electrical bistability *via* controlled energetics in donor–donor and donor–acceptor conjugated polymers

In this communication, we report for the first time benzodithiophene-based donor–donor and donor–acceptor 2D conjugated polymeric flexible memory devices with thermally/non-thermally recoverable WORM behaviors.

As featured in:

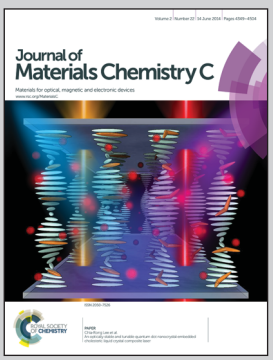

See Hsing-Lin Wang *et al.*, *J. Mater. Chem. C*, 2014, **2**, 4374.

ROYAL SOCIETY OF CHEMISTRY

www.rsc.org/MaterialsC

Registered charity number: 207890

Journal of Materials Chemistry C

COMMUNICATION

View Article Online
View Journal | View Issue

Cite this: J. Mater. Chem. C, 2014, 2, 4374

Received 7th January 2014
Accepted 20th March 2014

DOI: 10.1039/c4tc00039k

www.rsc.org/MaterialsC

Flexible memory devices with tunable electrical bistability *via* controlled energetics in donor–donor and donor–acceptor conjugated polymers†

Hung-Ju Yen,[a] Hsinhan Tsai,[a] Cheng-Yu Kuo,[a] Wanyi Nie,[b] Aditya D. Mohite,[b] Gautam Gupta,[b] Jian Wang,[c] Jia-Hao Wu,[d] Guey-Sheng Liou[d] and Hsing-Lin Wang*[a]

Flexible nonvolatile memory devices were fabricated from benzodithiophene-based donor–donor and donor–acceptor conjugated polymers with thermally/non-thermally recoverable memory behaviors.

In recent years, the applications of conjugated materials in optoelectronic devices such as light-emitting diodes,[1] solar cells,[2] thin film transistors,[3] electrochromic,[4] and memory devices[5] have attracted tremendous attention, due to their rich structural flexibility, low-cost, solution processability, large area fabrication, and three-dimensional stacking capability.[6] The emerging research on information storage in the form of high (ON) and low (OFF) current states in place of the amount of charges stored in silicon devices is to improve and/or enhance the superiority of higher data storage density, ease of miniaturization, longer data retention time, faster speed, lower power consumption, and cost-effective processing for practical use.[7] Polymeric materials with electrical bistability resulting from different electronic structures in response to the applied electric field begin to stand out conspicuously and have predominance in scaling down from micro-scale to nano-scale for memory devices. Thus, polymeric memory devices have been developed as a promising alternative to the conventional semiconductor-based memory devices.

In the initial stage of memory devices, polymers were used as polyelectrolytes and matrices.[8] Recently, design synthesis of polymers with specific structures that can provide desired electronic properties is a holy grail in developing efficient polymeric memory devices. For resistive type memory materials, several models of different mechanisms that can lead to electrical memory behaviours have been illustrated such as charge transfer (CT), conductive filament formation, and charge trapping/de-trapping.[5a] A few precedents using donor–acceptor systems have been demonstrated, including conjugated polymers (CPs),[9] non-conjugated polymers with donor–acceptor chromophores,[5b,d] and polymer nanocomposites.[10]

Among all donor–acceptor systems studied, CPs have been utilized to fabricate different types of memory devices, such as volatile dynamic random access memory (DRAM) devices, static random access memory (SRAM) devices, and nonvolatile write-once-read-many-time (WORM) devices. The electronic memory behaviors were found to be highly dependent on the molecular structure of the materials, which dictates properties such as the occurrence of charge transfer, turn-on voltage, and charge trapping.[5a] As nonvolatile memory devices that are capable of holding data permanently and being read repeatedly, WORM memory and flash-type memory devices are very desirable for ultralow-cost permanent storage of digital images because of the elimination of the need for slow, bulky, and expensive mechanical drives used in conventional magnetic and optical memory devices.[7] Basically, the WORM memory devices that function as conventional CD-R, DVD-R, or programmable read-only memory (PROM) devices can also be used as disposable memory devices in some niche areas, such as electronic labels and radio-frequency identification (RFID) tags.

Benzodithiophene (BDT)-based CPs have garnered considerable interest in the past few years due to their good performance in both organic field-effect transistors and solar cells.[11] In addition to the planar backbone, attaching different substituents to the BDT core offers the flexibility of fine-tuning the energy levels of the resulting polymers. The electronic structure could be easily modulated by adjusting the structure and affinity of the donor[2b] and/or acceptor moieties.[2c] Moreover, the emerged BDT-based two-dimensional CPs with alkylthienyl side chains could effectively increase the structure order,

[a]Physical Chemistry and Applied Spectroscopy (C-PCS), Chemistry Division, Los Alamos National Laboratory, Los Alamos, New Mexico 87545, USA. E-mail: hwang@lanl.gov

[b]Material Synthesis and Integrated Devices (MPA-11), Materials Physics and Applications Division, Los Alamos National Laboratory, Los Alamos, New Mexico 87545, USA

[c]Materials Science in Radiation & Dynamic (MST-8), Materials Science and Technology Division, Los Alamos National Laboratory, Los Alamos, New Mexico 87545, USA

[d]Institute of Polymer Science and Engineering, National Taiwan University, Taipei 10617, Taiwan

† Electronic supplementary information (ESI) available: Experimental section. See DOI: 10.1039/c4tc00039k

enhance processability, offer broader absorption spectra, and lower the HOMO energy levels, thus improving the photovoltaic properties of the device.[2a]

In this communication, we report for the first time thienyl BDT-based conjugated polymeric flexible memory devices with thermally recoverable WORM behaviors. A series of two-dimensional BDT-based CPs **CP1–CP4** with terthienyl/bithienyl side chains[12] was employed for memory device applications (Fig. 1a and b). The incorporation of terthienyl and bithienyl side chains allows the attachment of up to eight and six alkyl substituents per BDT repeating unit, respectively, which in turn produces organosoluble CPs with ease of processability, high molecular weight and improved film quality. Moreover, the electron-abundant bithiophene and electron-deficient benzothiadiazole units were chosen as part of the polymer backbone to construct donor–donor and donor–acceptor conjugated backbone systems.

The UV-vis absorption spectra of **CP1–CP4** are depicted in Fig. 1c and the optical energy band gap (E_g) is estimated by the onset wavelength. The smaller band gap energy of the benzothiadiazole-based polymers **CP3** and **CP4** (~1.60 eV) as oppose to bithiophene-based polymers **CP1** and **CP2** (~1.95 eV) is mainly due to the electron-deficient acceptor benzothiadiazole unit. Benzothiadiazole coupled with the electron-rich BDT core gives rise to a charge transfer characteristic accompanied by a persistent increase of the length of the polymer backbone and a smaller band gap energy.

The electrochemical properties of these polymers were investigated by cyclic voltammetry (CV, Fig. S1†). All the polymers exhibit clear oxidation and reduction couples at the onset potential (E_{onset}) of around 0.97 to 1.05 V and −0.91 to −1.27 V, respectively. The redox potentials of the polymers and their respective HOMO and LUMO (*versus* vacuum) are calculated and summarized in Table S1.† The similar HOMO levels for all polymers imply that the HOMO is basically localized on the donor BDT cores. In addition, the LUMO levels of the benzothiadiazole-based donor–acceptor polymers **CP3** and **CP4** are around −3.50 eV, which is 0.30 eV lower than that of the LUMO of bithiophene-based donor–donor polymers **CP1** and **CP2**. The results suggest that the introduction of an electron-deficient unit can effectively increase the electron affinity of benzothiadiazole-based polymers and lower LUMO levels.

The memory behaviors of these polymers were depicted by the current–voltage (*I–V*) curves on an ITO-coated PET (polyethylene terephthalate)/polymer CPs/Al sandwich device as shown in Fig. 2 and 3. Within the flexible device, CP films were used as active layers with Al and ITO as the top and bottom electrodes, respectively (Fig. 1b). Polymer film thickness was optimized around 160 nm and was used for all devices. Fig. 2 exhibits the *I–V* curve of donor–donor polymers **CP1** and **CP2**, which was measured with a compliance current of 0.01 A.

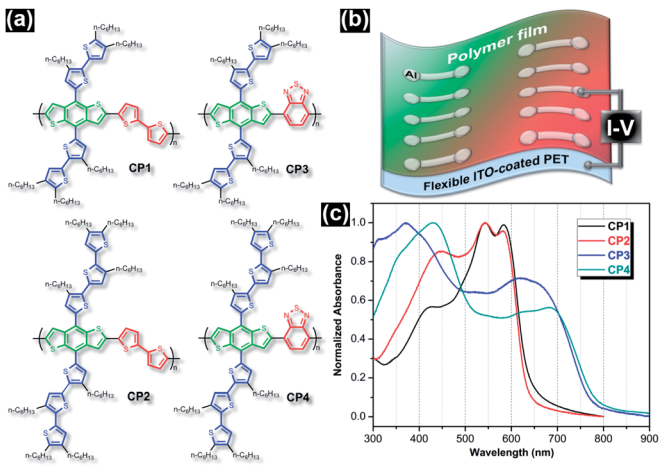

Fig. 1 (a) Chemical structures of CPs, (b) configuration of the flexible memory device, and (c) normalized absorption spectra of polymer thin films.

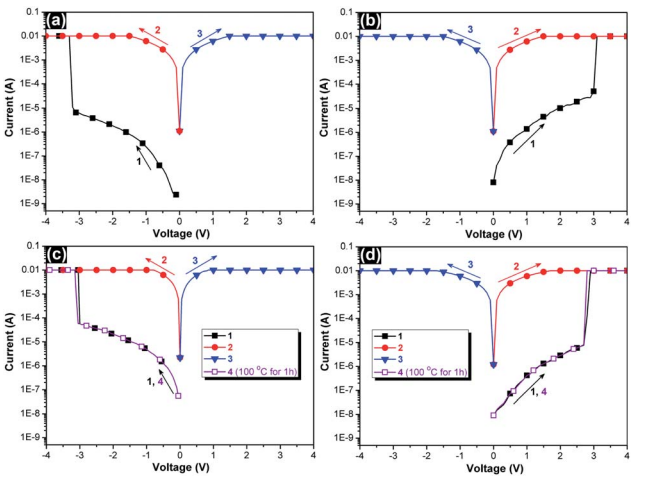

Fig. 2 Current–voltage (*I–V*) characteristics of the ITO/CPs (160 ± 10 nm)/Al memory device for donor–donor CPs with the first sweep performed negatively: (a) **CP1** and (c) **CP2** and positively: (b) **CP1** and (d) **CP2**.

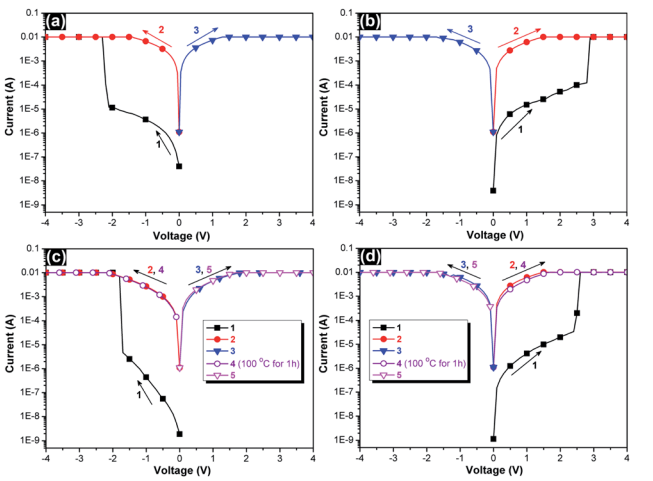

Fig. 3 Current–voltage (*I–V*) characteristics of the ITO/CPs (160 ± 10 nm)/Al memory device for donor–acceptor CPs with the first sweep performed negatively: (a) **CP3** and (c) **CP4** and positively: (b) **CP3** and (d) **CP4**.

Initially, the current of the as-fabricated device is low (defined as the OFF state). During the first negative sweep from 0 V to −4 V (Fig. 2a and c), the current increased gradually from 10^{-7} to 10^{-5} at a bias ranging from 0 to −3 V followed by a rapid increase to 10^{-2} A corresponding to the threshold voltage of around −3.0 V, indicating the transition from the OFF state to a high-conductivity (ON) state with an ON/OFF current ratio of 10^3 to 10^5. In a memory device, this OFF-to-ON transition can be defined as a "writing" process. The device remained in the ON state during the subsequent negative scan (the second sweep) and then positive scan (the third sweep). The memory device cannot be reset to the initial OFF state by applying a reverse electric field implying the non-erasable behavior. In addition, the ON state could also remain once the memory devices have been switched to the ON state at around 3.0 V (Fig. 2b and d), even after turn off power for an extended period of time (greater than a few hours). These results indicate that both **CP1** and **CP2** films exhibit nonvolatile WORM memory behaviors.

I–V curves of donor–acceptor polymers **CP3** and **CP4** are summarized in Fig. 3, revealing nonvolatile WORM behaviors with lower threshold voltages around −2.0 and 2.5 V for negative and positive sweeps, respectively. The slightly lower threshold voltages of **CP3** and **CP4** as oppose to **CP1** and **CP2** could be attributed to the donor–acceptor ability, which originates from the intra-chain charge transfer character. On the other hand, the turn on voltage of terthienyl-substituted polymers is 0.1–0.2 V lower than bithiophene-substituted polymers presumably due to their extended conjugation. This suggests strong correlation between the molecular structure and memory device properties. The threshold voltage, current and reversibility of the devices can be tailored through control synthesis of conjugated polymers with the backbone and side chains allowing fine-tuning of the energetics and degree of conjugation.

Taking into consideration the memory characteristics, we fabricated and investigated **CP4**-based memory devices with various thicknesses (Fig. S2†). We found that the device with a 120 nm thick **CP4** film always exhibits high conductivity in positive and negative voltage sweeps. As observed for the 120 nm thick films, both the 160 and 200 nm thick films exhibit WORM memory characteristics in positive and negative voltage sweeps. The results also suggest that the devices with thinner films have lower switching threshold voltages. Furthermore, the devices with a thickness higher than 240 nm only exhibit low conductivity in positive/negative sweeps and have no electrical switching behavior.[5d,13]

In order to demonstrate the feasibility of the switching properties of the flexible device, the device based on **CP1** was physically fixed to a vernier caliper from flat to bent conditions (Fig. 4a). The memory device was tested under severe bending at various radii of curvature, 11, 9, 7, and 5 mm, respectively, and the device remained intact. We also measured the switching memory behavior of the device under mechanical bending stress. Our results show reliable and reproducible memory properties under bending stress (Fig. 4b); throughout the bending process, we observe basically identical threshold voltage and similar current. Bending reveals no impact on

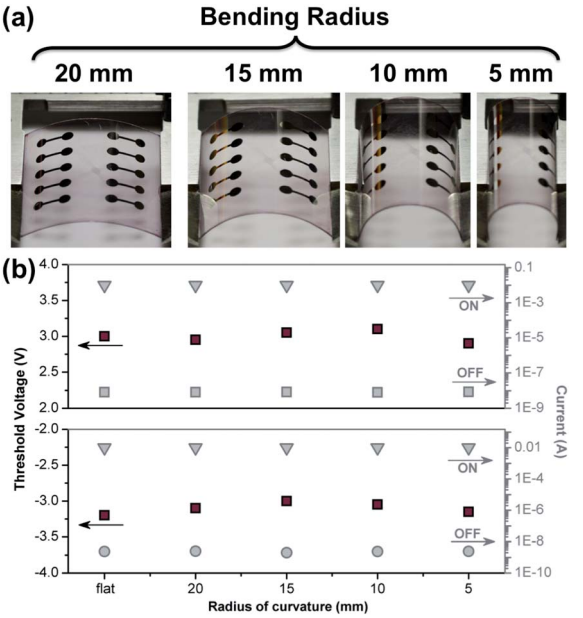

Fig. 4 (a) Appearance in various bent states and (b) variation of current and threshold voltage with different bending radii of the ITO/**CP1**/Al flexible memory device.

change in polymer chain conformations and electronic properties, which are two very important qualities for retaining the stability of flexible devices.

The molecular geometry and electronic structures of the polymers can help better understand the electronic process occurring inside the thin films. For gaining valuable insight into the memory behaviors of the polymeric devices, we calculated the molecular orbital and electric density contours of the basic units by molecular simulation. The molecular simulation on the basic unit of CPs was carried out by DFT/B3LYP/6-31 G(d) with the Gaussian 09 program. The charge density isosurfaces of the basic unit, the most energetically favorable geometry, the HOMO and LUMO energy levels of CPs are depicted in Fig. 5a. The mechanism of the electronic transition of CPs can be explained by the electric field induced CT effect between the donor and acceptor. The excitation of the donor units leads to the intra- or inter-molecular CT states. With the interaction between the donor and acceptor, the CT process gives rise to a charge separated and conductive state. For donor–acceptor polymers **CP3** and **CP4**, it is obvious that the benzothiadiazole unit contributes more to the LUMO while thienyl-BDT contributes more to the HOMO. Therefore, the memory devices based on both **CP3** and **CP4** exhibit very stable ON states once the devices were written since the high electron-accepting ability of the benzothiadiazole unit can stabilize the formed CT complex.

On the other hand, the HOMO energy levels of polymers **CP1** and **CP2** were distributed at the electron-donating thienyl-substituted BDT moieties along with the bithiophene backbone, indicating that the electron pull–push effect in donor–donor CPs is not obvious. Upon undergoing a transition from the HOMO to the LUMO, only a slight transition of the electron

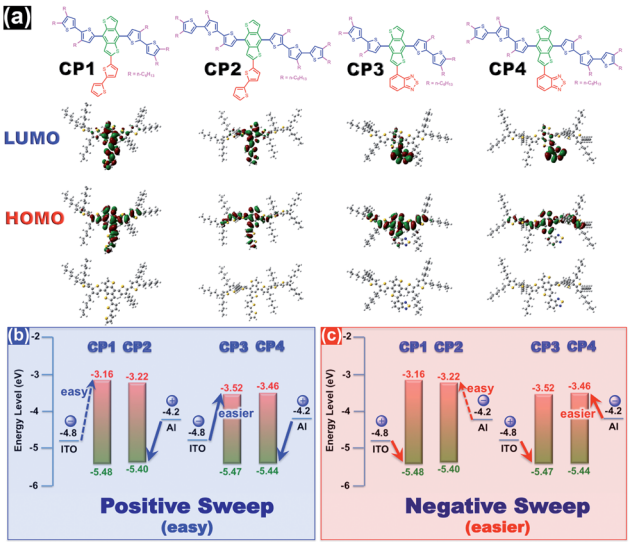

Fig. 5 (a) Calculated molecular orbitals and the corresponding energy levels of the basic units (BU) for CPs. HOMO and LUMO energy levels of CPs along with the work function of the electrodes for (b) positive sweep and (c) negative sweep.

density from the terthienyl/bithienyl side chains to the BDT–bithiophene backbone occurred. This transition would be easily recovered under a reverse voltage or even automatically revert to the OFF state, leading to the flash or DRAM memory behavior. However, since the LUMO energy level is a dominant factor for memory behavior, the electron could be located on the electron acceptor side (BDT–bithiophene), a new stable charge-separated state, and thus showing the WORM characteristics. It is important to note that there is a possibility to reverse the electron transfer process with external stimuli because bithiophene is not a strong acceptor.[14] Consequently, we carried out comparative studies of thermal stability between **CP2** and **CP4** with WORM memory behaviors, the results are summarized in Fig. 2c and d, 3c and d. After heating at 100 °C for 1 hour, the ON state of **CP2** recovered to the original OFF state due to a weaker charge-separated state. In contrast, the **CP4**-based memory device maintained its high conductivity after thermal treatment. These results are consistent with the proposed mechanism derived from molecular simulation and offer a design concept for thermally/non-thermally recoverable WORM memory devices, revealing great promise for advanced memory devices.

Based on our proposed mechanism, the energy diagram of CPs and the work function of the electrodes are shown in Fig. 5. When the positive sweep was conducted, the hole was easily injected from the top electrode Al to the HOMO of the polymer with an energy barrier of 1.2 eV between Al (−4.2 eV) and the HOMO (∼−5.4 eV) as shown in Fig. 5b. In contrast, during the negative sweep, the hole is easier to be injected from bottom electrode ITO into the HOMO of the polymer because of the smaller energy barrier (0.6 eV) between the work function of ITO (−4.8 eV) and the HOMO of the polymers (∼−5.4 eV), thus the memory device can be switched to the ON state at lower threshold voltages as oppose to the positive sweep (Fig. 5c). We use ease/easier to describe the properties of memory devices and the magnitude of the energy barrier between energy levels of polymers and metal work functions. The so-called "hard" typically refers to the devices that cannot be switched to the ON state. In addition, the donor–acceptor polymers **CP3** and **CP4** with lower LUMO energy levels can be switched to the ON state at lower threshold voltages in positive/negative sweeps due to the smaller energy barrier between the LUMO (∼−3.5 eV) and work function of ITO/Al as oppose to the donor–donor ones with higher LUMO levels (∼−3.2 eV). For **CP1** and **CP2**, the symmetrical *I–V* curves for positive and negative sweeps have comparable threshold voltages which can be explained by the electrical switching arising from the electric field-induced charge transfer rather than the hole injection process.[15] To further investigate the electrical switching characteristics of the memory devices, we analyzed the *I–V* characteristics of the OFF and ON states. The trap-limited space-charge limited conduction (SCLC) model was found to satisfactorily fit the *I–V* data for the OFF-state (Fig. S3†), while the Ohmic contact model was found to satisfactorily fit the *I–V* data for the ON-state (inset in Fig. S3†). This result indicates that a trap-limited SCLC mechanism is dominant in the OFF state and Ohmic conduction is dominant when the device is in the ON-state.[5d]

In summary, we have achieved fabrication and characterization of thermally recoverable flexible nonvolatile memory devices based on 2-D conjugated polymers. Combined theoretical and experimental studies of our donor–acceptor and donor–donor conjugated systems offer valuable insights to improve memory devices by rational design of molecular structures. We have demonstrated a strong correlation between resistive switching properties and the molecular structure through controlling the stability of the CT complex. Our results suggest the feasibility of tailoring the memory device properties through control synthesis of conjugated polymers with the backbone and side chains allowing fine-tuning of the energetics and the degree of conjugation. The novel thienyl BDT-based memory devices are flexible, thermally reversible, and have great promise for advanced organic electronics.

Notes and references

1 (*a*) Q. B. Pei, G. Yu, C. Zhang, Y. Yang and A. J. Heeger, *Science*, 1995, **269**, 1086–1088; (*b*) R. H. Friend, R. W. Gymer, A. B. Holmes, J. H. Burroughes, R. N. Marks, C. Taliani, D. D. C. Bradley, D. A. Dos Santos, J. L. Bredas, M. Logdlund and W. R. Salaneck, *Nature*, 1999, **397**, 121–128.

2 (*a*) L. J. Huo, J. H. Hou, S. Q. Zhang, H. Y. Chen and Y. Yang, *Angew. Chem., Int. Ed.*, 2010, **49**, 1500–1503; (*b*) D. Lee, E. Hubijar, G. J. D. Kalaw and J. P. Ferraris, *Chem. Mater.*, 2012, **24**, 2534–2540; (*c*) H. H. Cho, T. E. Kang, K. H. Kim, H. Kang, H. J. Kim and B. J. Kim, *Macromolecules*, 2012, **45**, 6415–6423.

3 (*a*) J. Rivnay, L. H. Jimison, J. E. Northrup, M. F. Toney, R. Noriega, S. F. Lu, T. J. Marks, A. Facchetti and A. Salleo, *Nat. Mater.*, 2009, **8**, 952–958; (*b*) H. Yan, Z. H. Chen, Y. Zheng, C. Newman, J. R. Quinn, F. Dotz, M. Kastler and A. Facchetti, *Nature*, 2009, **457**, 679–686.

4 (*a*) H. J. Yen and G. S. Liou, *Polym. Chem.*, 2012, **3**, 255–264; (*b*) H.-J. Yen, C.-J. Chen and G.-S. Liou, *Adv. Funct. Mater.*, 2013, **23**, 5307–5316.

5 (*a*) Q. D. Ling, D. J. Liaw, C. X. Zhu, D. S. H. Chan, E. T. Kang and K. G. Neoh, *Prog. Polym. Sci.*, 2008, **33**, 917–978; (*b*) S. J. Liu, P. Wang, Q. Zhao, H. Y. Yang, J. Wong, H. B. Sun, X. C. Dong, W. P. Lin and W. Huang, *Adv. Mater.*, 2012, **24**, 2901–2905; (*c*) S. G. Hahm, Y.-G. Ko, W. Kwon and M. Ree, *Curr. Opin. Chem. Eng.*, 2013, **2**, 79–87; (*d*) K. Kim, Y.-K. Fang, W. Kwon, S. Pyo, W.-C. Chen and M. Ree, *J. Mater. Chem. C*, 2013, **1**, 4858–4868.

6 A. Stikeman, *Technol. Rev.*, 2002, **105**, 31.

7 S. Moller, C. Perlov, W. Jackson, C. Taussig and S. R. Forrest, *Nature*, 2003, **426**, 166–169.

8 T. W. Kim, D. F. Zeigler, O. Acton, H. L. Yip, H. Ma and A. K. Y. Jen, *Adv. Mater.*, 2012, **24**, 828–833.

9 (*a*) H. C. Wu, A. D. Yu, W. Y. Lee, C. L. Liu and W. C. Chen, *Chem. Commun.*, 2012, **48**, 9135–9137; (*b*) H.-W. Lin, W.-Y. Lee, C. Lu, C.-J. Lin, H.-C. Wu, Y.-W. Lin, B. Ahn, Y. Rho, M. Ree and W.-C. Chen, *Polym. Chem.*, 2012, **3**, 767–777.

10 (*a*) X. D. Zhuang, Y. Chen, G. Liu, P. P. Li, C. X. Zhu, E. T. Kang, K. G. Neoh, B. Zhang, J. H. Zhu and Y. X. Li, *Adv. Mater.*, 2010, **22**, 1731–1735; (*b*) S. G. Hahm, N.-G. Kang, W. Kwon, K. Kim, Y.-G. Ko, S. Ahn, B.-G. Kang, T. Chang, J.-S. Lee and M. Ree, *Adv. Mater.*, 2012, **24**, 1062–1066.

11 I. F. Perepichka and D. F. Perepichka, in *Handbook of Thiophene-Based Materials*, John Wiley & Sons, Ltd, 2009.

12 C.-Y. Kuo, W. Nie, H. Tsai, H.-J. Yen, A. D. Mohite, G. Gupta, A. M. Dattelbaum, D. J. William, K. C. Cha, Y. Yang, L. Wang and H.-L. Wang, *Macromolecules*, 2014, **47**, 1008–1020.

13 T. J. Lee, C.-W. Chang, S. G. Hahm, K. Kim, S. Park, D. M. Kim, J. Kim, W.-S. Kwon, G.-S. Liou and M. Ree, *Nanotechnology*, 2009, **20**, 135204.

14 (*a*) C.-J. Chen, H.-J. Yen, Y.-C. Hu and G.-S. Liou, *J. Mater. Chem. C*, 2013, **1**, 7623; (*b*) G.-S. Liou, C.-J. Chen and J.-H. Wu, *Chem. Commun.*, 2014, **50**, 4335–4337.

15 (*a*) Y.-L. Liu, Q.-D. Ling, E.-T. Kang, K.-G. Neoh, D.-J. Liaw, K.-L. Wang, W.-T. Liou, C.-X. Zhu and D. S.-H. Chan, *J. Appl. Phys.*, 2009, **105**, 044501; (*b*) Y.-Q. Li, R.-C. Fang, A.-M. Zheng, Y.-Y. Chu, X. Tao, H.-H. Xu, S.-J. Ding and Y.-Z. Shen, *J. Mater. Chem.*, 2011, **21**, 15643–15654.

